‘L-CELL’ - A NOVEL DEVICE FOR PLATING PROCESS DIAGNOSTICS

Eugene Malyshev and Uziel Landau
L-Chem, Inc.
Shaker Heights, OH 44120 USA

Current technology for plating process characterization is based exclusively on the Hull-Cell or derivatives thereof, which provide only qualitative information based on visual inspection of the deposit. A novel device, which enables in a single automated and fast experiment to quantitatively determine the critical process parameters, while providing also visual sampling of the deposit at different, precisely determined, current densities is described. The device is based on simultaneously depositing metal at different, pre-determined current densities on a segmented cathode. The current/voltage data for each of the segments is recorded and analyzed by a software program, which provides complete process parameters and diagnostics. Examples including the effect of additives and the pH in the plating of copper and nickel are presented.

For more information contact:

Eugene Malyshev
L-Chem., Inc.
13909 Larchmere Blvd.
Shaker Heights, OH 44120
Phone: (216) 514-9998
Fax: (216) 932-4248
Email: cdw@L-Chem.com

Introduction and background

The performance of plating processes depends on the design of the plating cells, including racking and shielding, and on the proper selection of the operating conditions. The latter include the process chemistry, current density or voltage, flow, and temperature that must be selected to produce the desired deposit properties and thickness distribution. Traditionally, the design of plating processes has been considered an 'art' and involved costly and time-consuming 'trial and error' procedures, which depend mainly on experience rather than on precise engineering practices. This has led to inefficiency and long time-to-market, as well as losses due to inability to meet product specifications. In order to improve and optimize the design of the plating process, the plater relies mainly on a few available tools: (i) the Hull-Cell[1-5] that is widely used for process diagnostics and (ii) recently introduced electroplating CAD software (e.g., Cell-Design© [6]), that eliminates 'trial and error' from cell-design and optimization. Both those 'tools' suffer, however, from limitations, as discussed below, which the L-Cell addresses.

The Hull-Cell - Comprehensive plating bath analysis is difficult, particularly since the process performance critically depends upon minute amounts of plating additives that are often consumed by the process, and contaminants that build-up in the bath. These often cannot be directly analyzed, yet they strongly affect the process. Electroplaters widely rely on semi-empirical observations using a largely *qualitative* device, the 'Hull-Cell', to control their process. The Hull-cell consists of a small prismatic container with vertical insulating sidewalls, an anode, and a plated panel that is placed in a slanted orientation with respect to the anode and the cell walls. Because of the cell configuration the current density across the panel and the corresponding deposit thickness vary: the highest current density is near the obtuse angle; the lowest, next to the acute angle. After plating, the panel is visually inspected, comparing the deposit appearance at different current densities to expected values. Since only the total current is measured, users apply a scale on which the current density is indicated as a function of position[7].

A major deficiency of the Hull-cell is that the indicated current density is only an approximation. This approximation is intrinsic to the Hull-cell because the current distribution depends not only on the cell geometry, but also varies with the type of plating solution used. The curves displayed in Fig. 1 show the computed current density distributions in typical electrolytes as modeled by Cell-Design© [6], in comparison to the corresponding values indicated by the Hull cell scale. As noted, even for very common electrolytes, significant differences (exceeding 25%) exist at low and high current densities. Additional discrepancies will show up due to variations in the electrolyte temperature, ionic concentrations, conductivity, additive concentration, contaminants and by-products which are not accounted for. More recently, Kadija *et. al.*[7] introduced the 'hydrodynamically modulated Hull cell', designed to provide better quantified mass transport. This cell suffers from the same deficiencies that apply to the Hull cell, i.e., it provides a distribution that depends on the electrolyte type and composition, and therefore any provided current density scales are inherently inaccurate. Another similar cell that has been recently introduced in Europe by Landolt and Madour has identical features and suffers from the same shortfalls. None of the described cells provide any *quantitative* information concerning the physical and/or chemical parameters of the process.

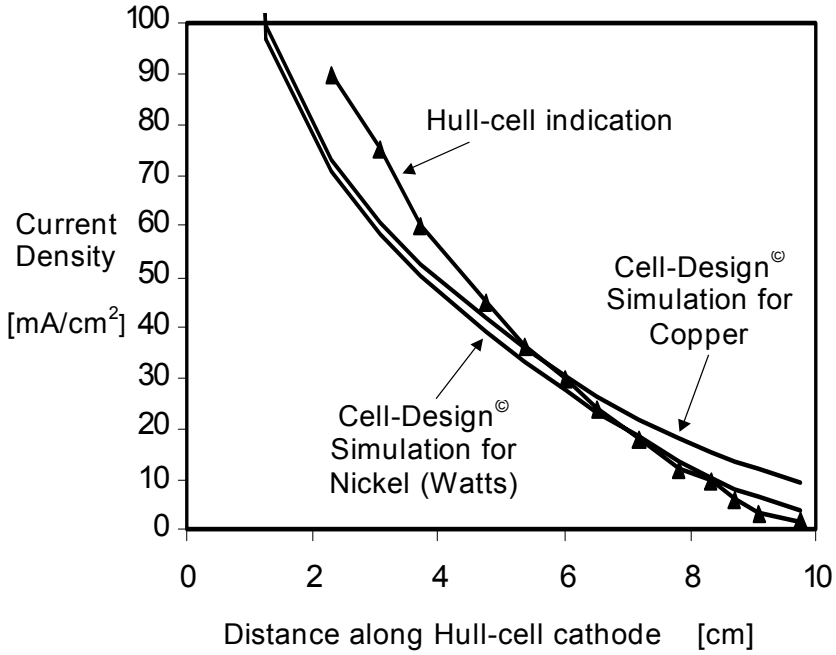

Fig. 1: Comparison between current distributions as indicated by the 'Hull-Cell' scale and Cell-Design©[6] simulations for the plating in a Hull-cell of copper from acidified copper sulfate, and nickel from a 'Watts' type bath.

***Computer-Aided–Design (CAD)* Software –** The more sophisticated plating shops have recently started to migrate towards more advanced modeling tools, primarily computer-aided design and engineering (CAD/CAE) software, e.g., L-Chem's 'Cell-Design'[6]. Such software provides a convenient and fast route to predictive cell and process design thus eliminating the need for costly 'trial and error', yet its application requires data that in many cases is not readily available.

As shown in Fig. 2, CAD modeling requires, in addition to specification of the cell configuration and operating conditions, also the process properties. The latter include the electrode reaction parameters and the electrolyte transport properties. The main barrier for wider dissemination of CAD tools has been the lack of available process properties data that the software requires as input. Availability of the process parameters (e.g., the conductivity, and kinetics constants) is an essential prerequisite for the modeling; yet this data is typically not available.

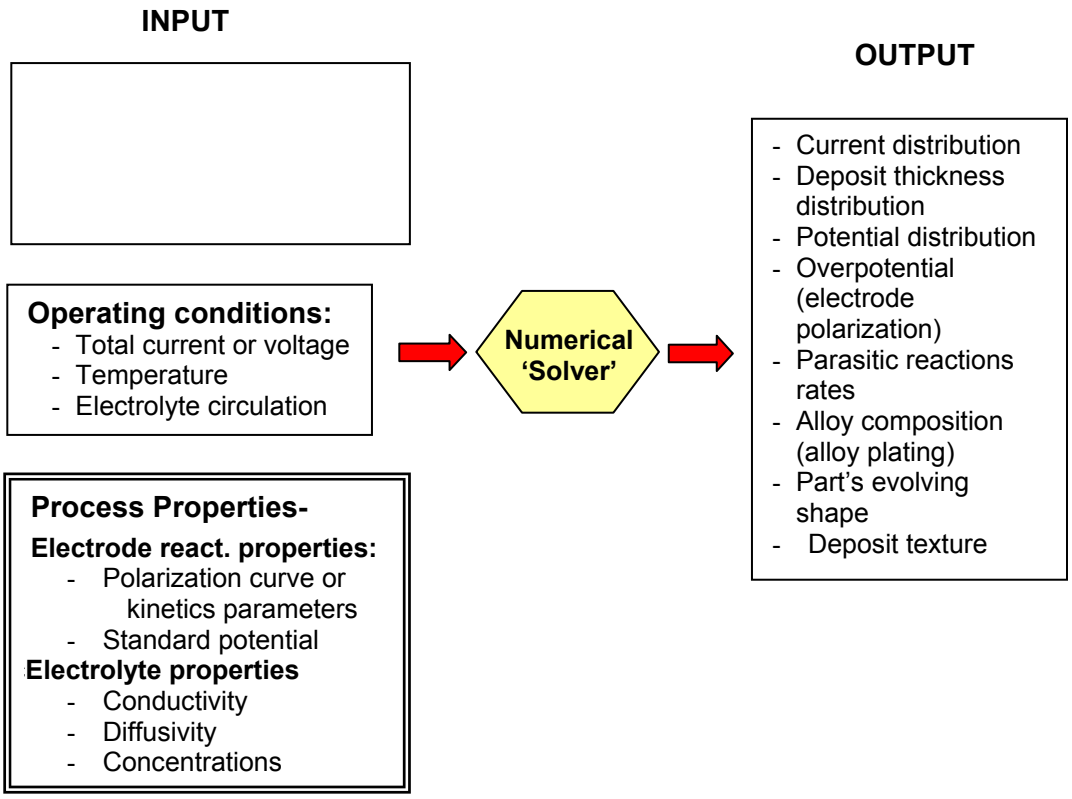

Fig. 2: A diagram showing the major input and output parameters associated with CAD analysis of electrochemical cells. The process properties listed at the lower left are particularly hard-to find for most commercial electrolyte formulations.

Generating this data is an onerous task, particularly considering the numerous commercial electrolyte formulations. The data can be grouped into two major categories:

(i) Data related to the electrode processes, which typically involve complex steps that are difficult to unravel. Their characterization can, however, be achieved without detailed mechanistic knowledge by specifying the global electrode kinetics. This requires measuring the polarization curve, which describes the dependence of the electrode overpotential on the current density. The polarization curve is commonly represented in terms of the 'Butler-Volmer' equation relating the current density, i, to the overpotential, η, incorporating three parameters: the exchange current density [i_0] and the anodic [α_A] and cathodic [α_C] transfer coefficients[9,10].

$$i = i_0 \left\{ e^{\frac{\alpha_A F}{RT}\eta} - e^{-\frac{\alpha_C F}{RT}\eta} \right\} \qquad [1]$$

(ii) Ionic transport in the electrolyte involves diffusion, migration and convection. Its simulation requires the 'integral' diffusion coefficient of the reactant, which can be measured on a rotating disk electrode[11, 12].

The literature typically offers rate constants for solely pure elements. Practical processes employ complex chemistries, incorporating additives and complexing agents that strongly affect the deposition kinetics[13-16]. It is therefore required in almost all practical situations to measure the parameters for the given system. Such measurements, however, require special cells, e.g., conductivity cells coupled with a high frequency analyzer for conductivity measurement, and a rotating disk electrode for measurements of diffusivity. The empirical rate constants i_0, α_A and α_C are typically obtained by conducting a sweep of a current-potential scan in cells that must provide (a) a uniform current density (b) uniform and tractable transport rates (c) means of detecting the ohmic and concentration overpotentials, and (d) a three electrode system incorporating a reference electrode coupled with costly power supply ('potentiostat') capable of three-electrode measurements. The experimental set-up is expensive, the process of generating the data is time consuming, and requires expertise.

The L-Cell: Description and Principles of Operation

Output from the L-Cell - The L-Cell is a dual purpose device: **(a)** The L-Cell provides essentially all the data needed to quantitatively characterize the electrochemical system from a single fast deposition experiment carried out automatically. This data can be used either for CAD modeling, or for quantitative process diagnostics. The data includes the polarization curve and its associated kinetics constants (i_0, α_A, α_C), as well as the electrolyte conductivity. In alloy deposition, when the segmental compositions are analyzed (in separate testing) the kinetics for the entire alloy system can be obtained from a single experiment. Such alloy data cannot be generated by the corresponding current/potential scanning experiment. The current efficiency, which typically varies with the current density, can be determined by comparing the precisely measured segmental currents to measurements of the corresponding deposit thickness or the weight of the different plated 'patches'. **(b)** The L-Cell provides multiple discrete electrode sites at which electrochemical reactions proceed simultaneously at different and, unlike the Hull-Cell, precisely measured rates producing multiple discrete deposit patches which can later be studied visually and analytically (e.g., by x-ray). The device thus provides a precise correlation between the appearance of the deposit and the current density.

Principle of operation - The L-Cell measurements are based on simultaneously plating a number of discrete cathodic segments, each at a different and precisely pre-determined current density, while measuring and recording the corresponding overpotentials. The polarization curve is then constructed by plotting the segmental current densities vs. their corresponding overpotentials, interpolating between the discrete points. This method of generating a polarization curve is fundamentally different from the classical technique of measuring electrode kinetics where the

current or the potential are scanned with time. Using the L-Cell, one no longer needs a costly potentiostat with scanning capability. Furthermore, since no transient measurements are involved, unsteady-state effects that mandate slow scanning are eliminated, and the entire polarization curve can be constructed within a few minutes from a number of points generated simultaneously. An important benefit is that a number of discrete deposit patches are generated at precisely known current densities. Those can be analyzed for appearance and composition. Obviously, such samples cannot be generated during a conventional potential or current scan, where the substrate is plated under varying conditions. In comparison to the Hull Cell, the deposit patches are generated at precisely known current densities. Furthermore, process diagnostics need no longer be based on qualitative visual inspection of the deposit appearance as provided by the Hull-Cell, but can instead be based on quantitative data. Changes in polarization curves, kinetics constants, or the electrolyte conductivity which are measured and recorded by the L-Cell provide a quantitative process diagnostics.

Description of the device - The L-Cell consists of two major components: (i) The plating fixture and (ii) the electronic control box. The tabletop plating fixture, shown in Figs. 3 and 4, consists of a small rectangular cell [15 cm (6 inches) long by 2.5 cm (1 inch) wide by 7.5 cm (3 inch) high] into which 40 cm^3 [40 ml] sample of the tested solution is poured and a specially patterned test panel is inserted and plated. The test panel, shown in Fig. 5, is a customized printed circuit board, consisting of an insulating substrate onto which a conductive metal stripe pattern is printed. The lower, broader pads of the pattern (each about 1 cm^2 in area) are plated; the upper, narrower stripes provide means for feeding the current to the plated pads. Two of the pads, one at the front end and the other at the back end of the electrode array, are not be plated and are used instead as reference and sensing electrodes. The metal pattern is made of copper. To avoid issues of mixed potentials when characterizing the plating of metals other than copper, test panels, pre-plated with metal matching the type of the tested plating solution, are provided. These include nickel, zinc, chromium, lead, and gold. Users may also pre-plate their copper patterned substrates with any other desired metal.

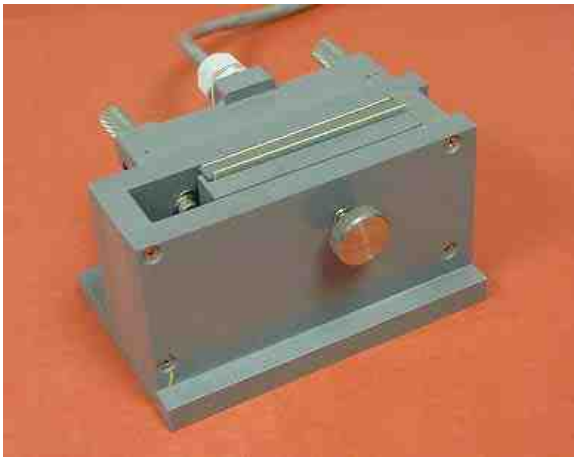

Fig. 3: The L-Cell. The device consists of a small container into which 40 cm^3 of the tested electrolyte are poured and a template (Fig. 5) with a segmented electrode is inserted and plated. The bolt in front seals the plated template against the mask (not visible) that assures a uniform (but different) current density across each segment. The cable in the back provides the current and transfers the voltage measurements to the control box (Fig. 4)

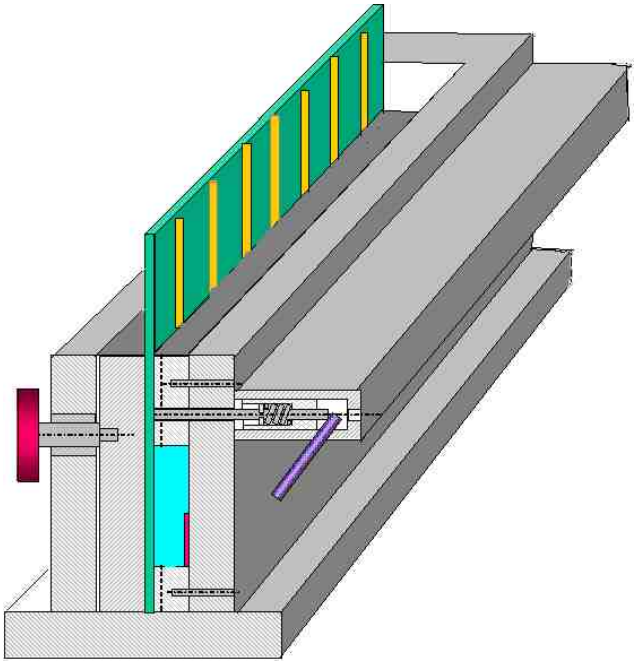

Fig. 4: Isometric cross-section (schematic) of the 'L-Cell'. The test panel consists of a printed circuit board that is inserted from the top and pressed by a screw driven back-plate against a mask. Spring loaded contacts feed the current to the printed contact stripes above the electrolyte level. Only the pads facing the anode (bottom right of the cavity) which are exposed to the electrolyte through slots in the mask are plated.

Fig. 5: The L-Cell plating template. Nickel plating on the pads is noted. The two pads at the edges serve as reference electrodes. The copper stripes feed the current to the pads. The larger copper pads on top serve as contacts.

The test panel is pressed by a screw-driven back-plate against a mask with a slot pattern. The slots expose predetermined regions of the metal pattern on the test panel to the plating current. The anode is a platinized titanium mesh that provides high area for easy removal of oxygen bubbles that are formed in the anodic reaction. The cavities through which the electrode segments are exposed to the electrolyte were designed such that the current density within each of the distinct plated regions is almost uniform (but different on each pad), irrespective of the plating electrolyte or the current density, as shown in the sample simulation by 'Cell-Design' depicted in Fig. 6.

The connector assembly mounted on the plating cell provides means for feeding the current separately to each of the plated segments, and the sensing voltage to the reference electrodes. The connector assembly consists of rod contacts that are pressed against the metal stripes on the test panel, such that a different rod makes contact with each of the metal stripes, enabling the feed of a different magnitude current to each of the plated pads. A multi-conductor cable feeds the currents from the connector assembly to the electronic control box (Fig. 7). The electronics control box provides control of the segmental currents such that they are maintained at different fixed values, irrespective of the electrolyte being tested. The control box allows the user to optionally select current and voltage ranges different from the default values for the test. The electronics control box also incorporates the data acquisition system that measures the segmental currents and voltages and feeds those via a serial cable to a computer for analysis and display.

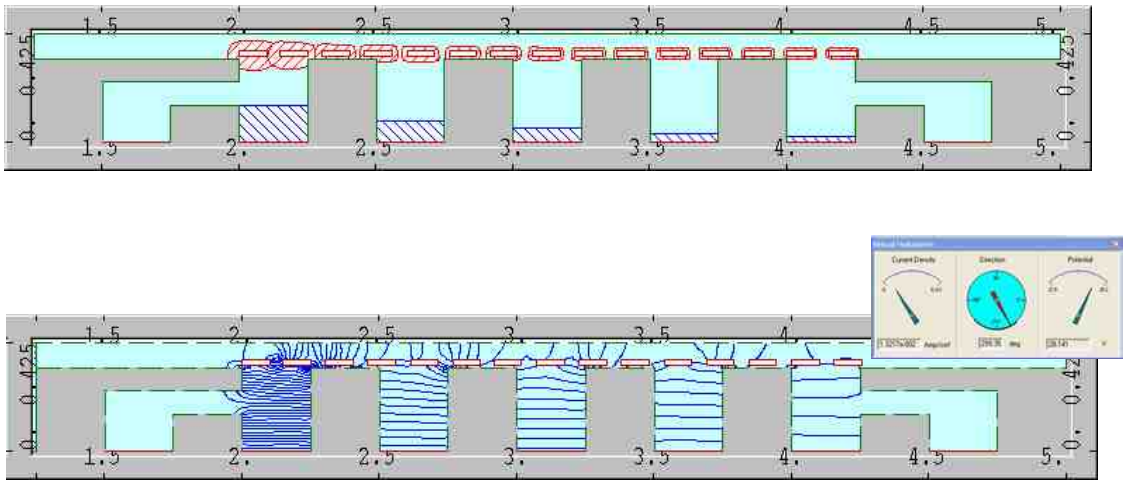

Fig. 6: ***Top:*** Current distribution in the 'L-cell' (cross-section) as simulated by Cell-Design software[6]. The crosshatched blue region corresponds to the magnitude of the cathodic current density, while the red region indicates the anodic current. As noted, the current density lines are flat within each plated region and vary considerably between the patches, starting with a very low current density at the right and increasing, stepwise, to a high current density on the left. The electrode segments at both ends do not plate and serve as reference electrodes. ***Bottom:*** Potential map in the cell. The virtual digital multimeter in the upper right indicates interactively the current density (magnitude and direction) and the voltage at any position within the cell.

Fig. 7: The electronic control box (left) and the plating fixture (right) of the L-Cell

An accompanying software program computes and displays the polarization curve (i.e., a plot of segmental current densities vs. the segmental overpotentials). The computations are based on conducting voltage balances between the different cathodic segments, the reference electrode, and the anode. The program also extracts the needed parameters (i_0, α_A, α_C, κ) from the recorded data. The computed parameters and the polarization curve showing the measured experimental points are displayed graphically and numerically. The data can be used in two ways: (i) it can be used for CAD modeling providing essential and typically non-available polarization data, which can be directly linked with e.g., Cell-Design's database; and (ii) it can provide quantitative and precise diagnostics of the process. Here, the polarization curve and the kinetics constants can be compared with standards, best measured in the fresh electrolyte. Deviations from the standards indicate depletion, contamination, and/or aging, and the bath can be then treated accordingly. A third deliverable of the L-Cell test is the plated template that can be inspected visually for deposit appearance at five different current densities. Measuring the deposit thickness on each of the pads, the current efficiency can be determined as a function of the current density. Other tests of the deposit properties, e.g., hardness, purity, etc., can also be conducted at five different current densities. In alloy plating, deposit patches that have been plated at five different current densities are available for compositional analysis, providing the polarization curves of the single components as they interact in the alloy system.

Sample Results and Discussion

The recorded polarization data has been correlated with equation [2] which represents the Butler-Volmer equation corrected for mass transport limitations:

$$i = i_0\left(1-\frac{i}{i_L}\right)\left\{e^{\frac{\alpha_A F}{RT}\eta} - e^{-\frac{\alpha_C F}{RT}\eta}\right\} \qquad [2]$$

i_L is the limiting current given by:

$$i_L = \frac{nFDC_B}{(1-t_{Cu})\delta_N} \qquad [3]$$

Here, n, F and D are the number of electrons transferred in the electrode reaction, Faraday's constant, and the plated ion diffusivity, respectively. C_B is the reactant bulk concentration, t_+ its transport number, and δ_N is the equivalent mass transport boundary layer thickness. For the non-agitated L-Cell, δ_N has been measured by the limiting current technique and found to be: δ_N = 120 μm (4724 μ-inches). To allow for convenient correlation of the data, the polarization curve [2] has been plotted in terms of:

$$i_K \equiv \frac{i}{\left(1-\frac{i}{i_L}\right)} = i_0 \left\{ e^{\frac{\alpha_A F}{RT}\eta} - e^{-\frac{\alpha_C F}{RT}\eta} \right\} \qquad [4]$$

i_K as defined by Eq. [4] is the 'pure kinetics' (= mass transport independent) current density. Clearly, when the agitation rate is high and $i \ll i_L$, i approaches i_K. Furthermore, it can be shown that whenever a cathodic reaction is conducted under moderate or high polarization (corresponding to the situation where $|i| \gg i_0$), the last term on the right of Eq. [4], representing the cathodic branch of the reaction, is dominant over the left term within the brackets. Consequently, Eq. [4] can be simplified:

$$i_K = -i_0 \left\{ e^{-\frac{\alpha_C F}{RT}\eta} \right\} \qquad [5]$$

A straight line is expected when plotting $\log(i_K)$ vs. the overpotential η,. The slope of the line is $\alpha_C F/RT$ from which α_C can be determined and the intercept is $\log(i_0)$.

Copper plating from a slightly acidified copper sulfate electrolyte containing 100 ppm PEG – Copper plating electrolyte consisting of 0.5 M $CuSO_4$, slightly acidified with sulfuric acid to pH=2 with 70 ppm chloride and 100 ppm polyethylene glycol (PEG) was tested in the L-Cell. The PEG is a commonly used additive in copper plating known to polarize the electrode and enhance leveling. The chloride is a brightening agent and also enhances the PEG polarization effect. The limiting current was calculated and measured to be i_L = 50 mA/cm^2. The polarization curve, plotted in terms of i_K vs. η is shown in Fig. 8:

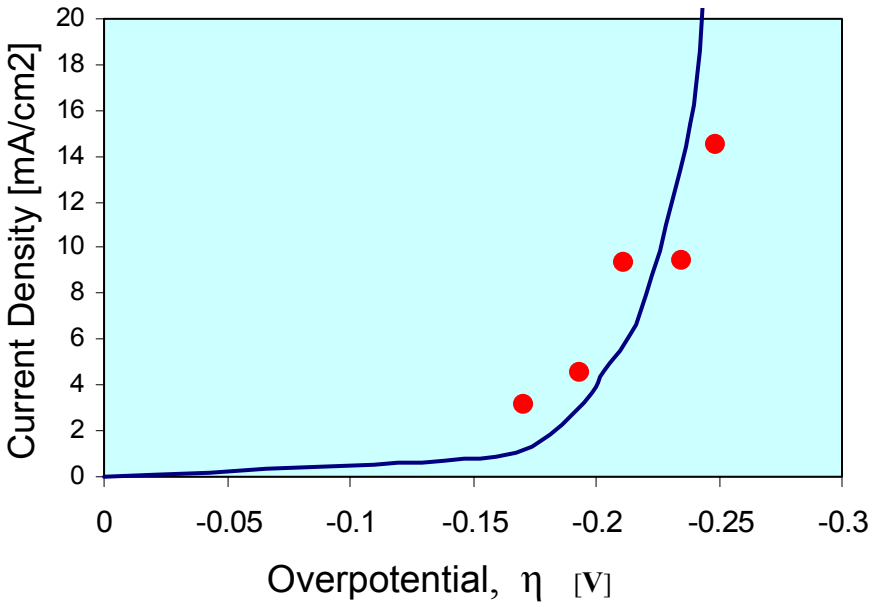

Fig. 8. Polarization data for Cu electrolyte with 100 ppm PEG. The red circles correspond to data obtained in the L-Cell. The solid line represents polarization data obtained using a rotating disk electrode system and a potentiostat. Good agreement between the L-Cell results and conventional polarization is noted.

Also shown in Fig. 8, as a solid line, is a polarization curve obtained for the identical solution using the conventional technique of polarizing a rotating disk electrode (Pine Instruments) using a potentiostat (EG&G). The disk was rotated at 50 RPM. The corresponding mass transport boundary layer thickness was 60 μm, yielding a limiting current of about 100 mA/cm^2. The mass transport limitation was accounted for using equations [3] and [4]. The overpotential was recorded using a copper reference electrode and compensated for the ohmic loss in the electrolyte using the resistance as determined by Cell-Design[6], simulation of the rotating disk electrode experimental set-up. Excellent agreement is noted between the L-Cell results (circles) and the conventional measurements using the rotating disk electrode and the potentiostat (solid line). The agreement is even more pronounced when the same data was plotted as log i_K vs. the overpotential in Fig. 9. This linear plot allows to quantitatively extract the kinetics parameters for the system, which were found to be: $\alpha_C = 0.6$ *and* $i_0 = 5x10^{-5} A/cm^2$. These values are in the expected range and indicate inhibition of the deposition reaction due to the PEG. This becomes apparent when compared below to polarization experiments conducted in the L-Cell for a similar copper sulfate electrolyte that did not contain the organic additive (PEG).

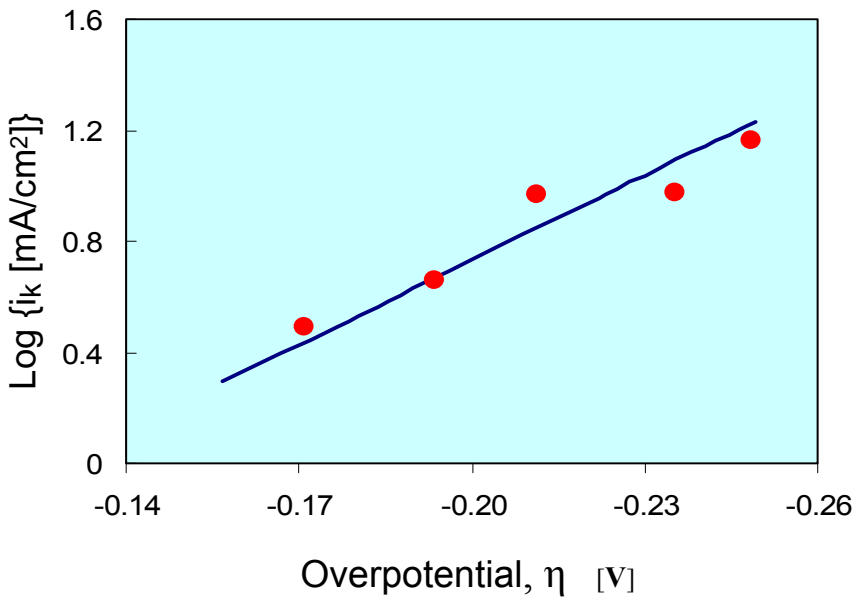

Fig. 9. Polarization data for Cu electrolyte with 100 ppm PEG correlated in terms of log i vs. the overpotential. The circles correspond to data obtained in the L-Cell. The solid line corresponds to polarization data obtained using a rotating disk electrode system and a potentiostat. The data correlates with the kinetics parameters: $\alpha_C = 0.6$ *and* $i_0 = 5x10^{-5} A/cm^2$.

Copper plating from a slightly acidified copper sulfate electrolyte – No organic additives - Copper plating electrolyte consisting of 0.5 M $CuSO_4$ slightly acidified with sulfuric acid to pH=2 with 70 ppm chloride was tested in the L-Cell. The limiting current was calculated and measured to be i_L = 50 mA/cm^2. The polarization curve, plotted in terms of i_K vs. the overpotential, η, is shown in Fig. 10. In order to extend the data range, the L-Cell testing was performed at two different current density settings, low and high, corresponding to the blue and red circles in Fig. 10. Clearly, the two data sets mesh well together. The solid line in Fig. 10 represents a polarization curve with the parameters: $\alpha_C = 0.5$ *and* $i_0 = 6x10^{-4} A/cm^2$. These parameters were determined from the semi-logarithmic polarization plot displayed in Fig. 11, where the linear least square fit of the data, represented by the straight line, indicates those values.

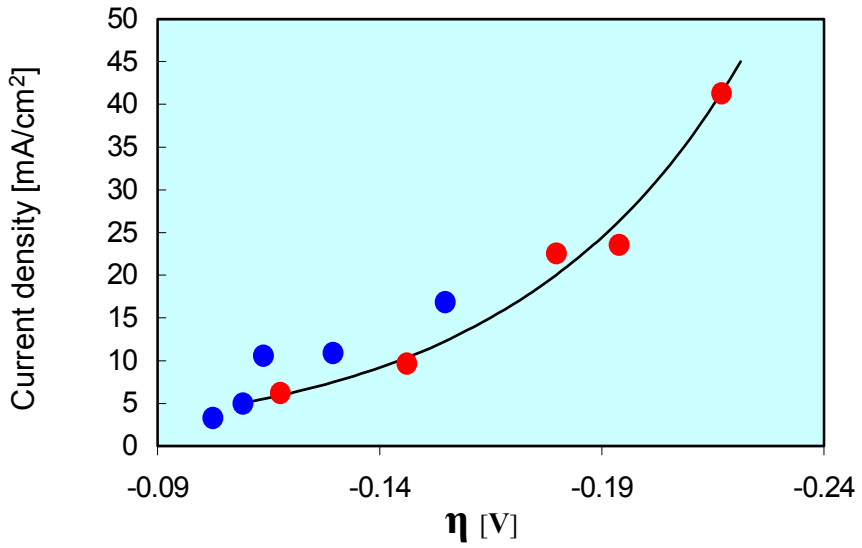

Fig. 10. Polarization data for Cu electrolyte without organic additives.. The solid circles correspond to data obtained in the L-Cell at two different current density ranges. The solid line represents a polarization line with the kinetics parameters: $\alpha_C = 0.5$ *and* $i_0 = 6x10^{-4} A/cm^2$.

This 'pure' copper kinetics data is in general agreement with data reported in the literature[19]. The slope of the line, indicating $\alpha_C = 0.5$ matches the most common value reported. There is a wide distribution of reported values[19] for i_0 (determined from the intercept on the ordinate when $\eta = 0$ in Fig. 11). Our value of 0.6 mA/cm^2, is somewhat in the low range, but this may be due to the presence of 70 ppm chloride in our electrolyte.

Using the L-Cell to detect variations in organic additives - Comparing the copper polarization kinetics in the PEG containing electrolyte to the analogous parameters in an identical solution, which, however, does not contain PEG, demonstrates the effectiveness of the L-Cell in diagnosing electrolyte contamination or additives consumption. The enhanced polarization due to the presence of the 100 ppm PEG is clearly noticed in Figs. 12 and 13.

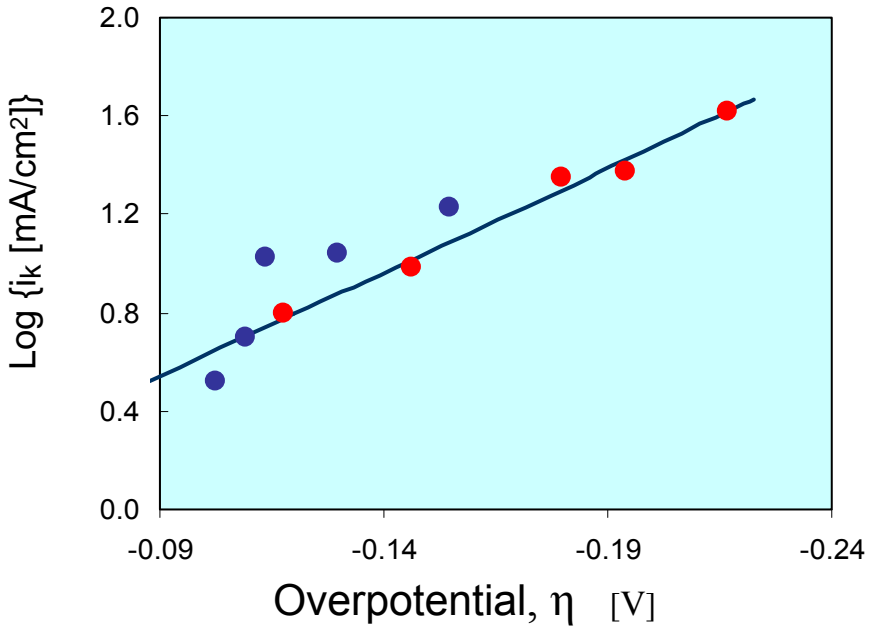

Fig 11. Polarization data for Cu electrolyte without organic additives correlated in terms of log i vs. the overpotential. The circles correspond to data obtained in the L-Cell at two different current density ranges. . The solid line represents a polarization line with the kinetics parameters: $\alpha_C = 0.5$ and $i_o = 6x10^{-4} A/cm^2$.

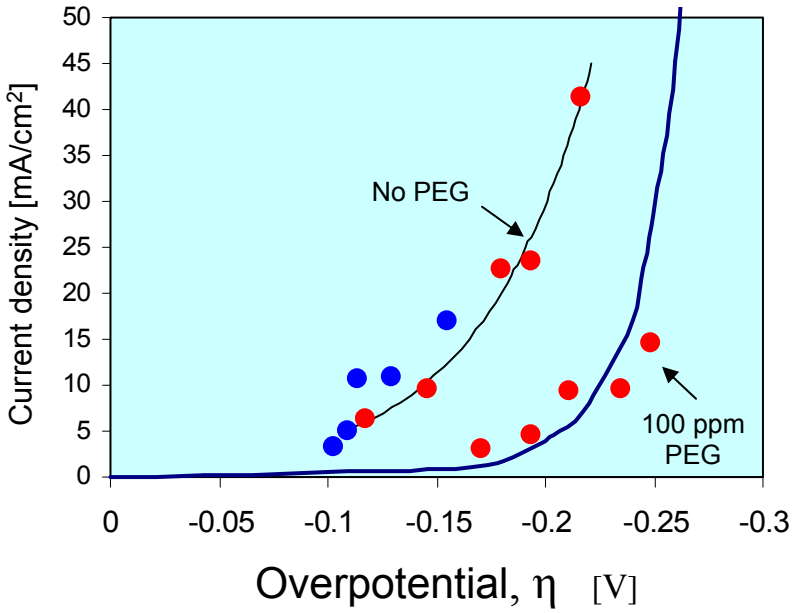

Fig 12. Comparison of copper polarization curves obtained in the L-Cell in the presence (right) and absence (left) of 100 ppm PEG.

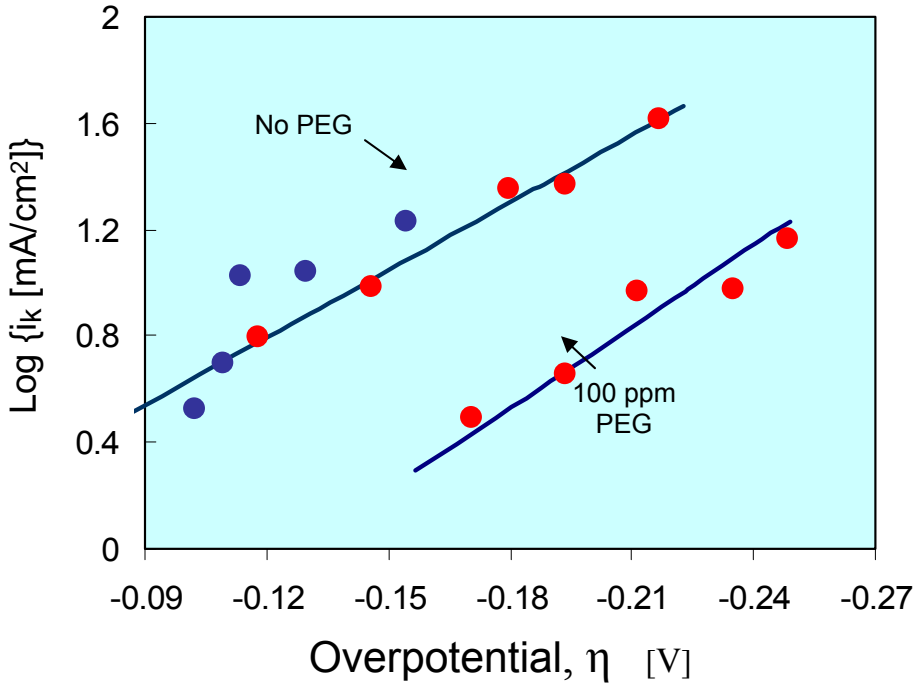

Fig 13. Comparison of copper polarization curves obtained in the L-Cell in the presence (right) and absence (left) of 100 ppm PE. A semi-logarithmic presentation yields as expected linear dependence.

Kinetics of a Watts Nickel Electrolyte - A Watts Nickel electrolyte, made of 225 g/L $NiSO_4$ * $6H_2O$; 60 g/L $NiCl_2$ * $6H_2O$; 35g/L H_3BO_3; pH ~ 3 without organic additives was tested in the L-Cell. To observe the nickel polarization across a broader current and potential range, four different current density ranges were tested as indicated by the differently colored circles in Figs. 14 and 15. Clearly, all the separate data-sets mesh into a single line. Due the higher nickel concentration (in comparison to the previously analyzed copper) the nickel limiting current was about 120 mA/cm^2. The measured current was corrected according to equations [3] and [4] to compensate for mass transport effects. The polarization data recorded by the L-Cell, is presented in terms of the 'kinetic current density', i_K, vs. the overpotential in Fig. 14. The same data is plotted in terms of log i_K vs. the overpotential in Fig. 15. As expected, a linear dependence is observed indicating the kinetics parameters: $\alpha_C = 0.18$ and $i_0 = 6.5 \times 10^{-5}$ A/cm^2. As expected, the nickel displays significantly higher polarization than that of copper.

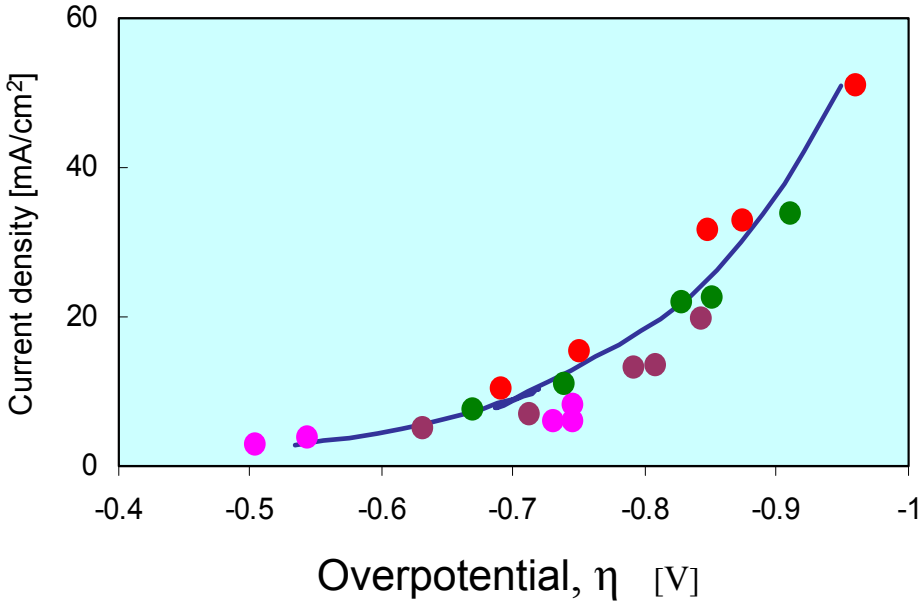

Fig. 14. Polarization data for Nickel Watts bath. The solid circles correspond to data obtained in the L-Cell at four different current density ranges. The solid line represents a polarization line with the kinetics parameters: $\alpha_C = 0.18$ *and* $i_0 = 6.5x10^{-5} A/cm^2$.

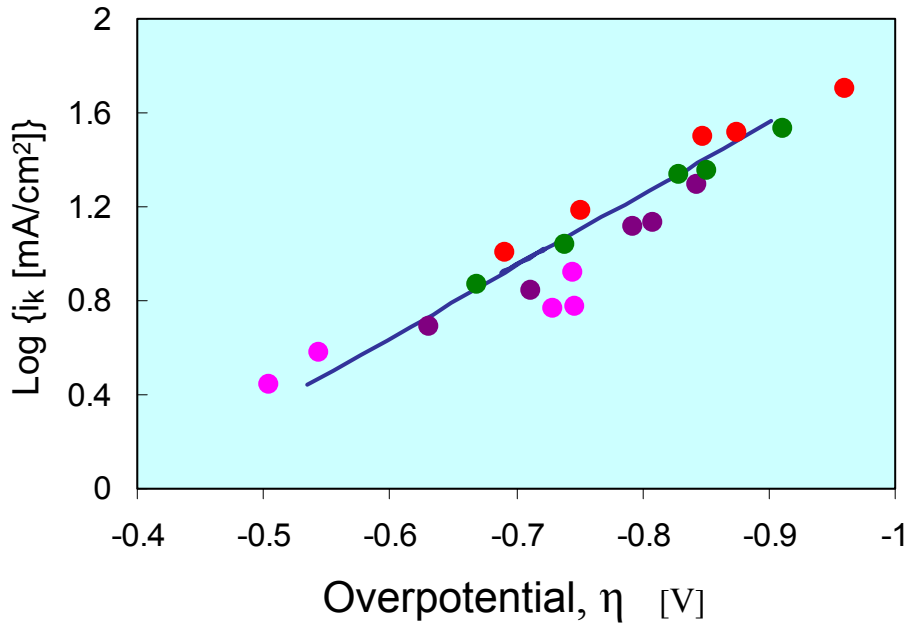

Fig. 15. Polarization data for Nickel Watts bath correlated in terms of log i vs. the overpotential. The circles correspond to data obtained in the L-Cell at four different current density ranges. The solid line represents a polarization line with the kinetics parameters: $\alpha_C = 0.18$ *and* $i_0 = 6.5x10^{-5} A/cm^2$.

References

1. R. O. Hull, "Current Density Range Characteristics--Their Determination and Application", *Proc. Amer. Electroplaters Society*, 27 (1939), pp. 52-60.
2. Walter Nohse, et al., "The Investigation of Electroplating and Related Solutions with the Aid of the Hull Cell", Robert Draper, Ltd., Teddington, England (1966), pp. 17-25.
3. U.S. Patent # 2149344, R. O. Hull, issued March 1939
4. U.S. Patent # 2760928, Ceresa, issued August, 1956.
5. U.S. Patent # 2801963, R. O. Hull et. al, issued August, 1957
6. Cell-Design©, Software for computer-aided-design of electrochemical cells, L-Chem Inc,, 13909 Larchmere Blvd., Shaker Heights, OH 44120. Website: www.L-Chem.com
7. "Hull cell scale", McGean-Rohco, Inc., 2910 Harvard Ave, Cleveland, Ohio, 44105
8. Kadija, J.A. Abys, V. Chinchankar, and H. K. Straschil , *"Hydrodynamically controlled Hull-Cell", Plating and Surface Finishing*, July 1991
9. J. S. Newman, *"Electrochemical Systems*", Prentice-Hall, Inc., Englewood Cliffs, N.J. (1973).
10. J. Bard and L. Faulkner, "*Electrochemical Methods"*, John Wiley and Sons, N.Y. 1980.
11. Venjamin Levich, "*Physicochemical Hydrodynamics*", Prentice-Hall, Englewood Cliffs, NJ, 1962.
12. Uziel landau, "*Determination of Laminar and Turbulent Mass Transport Rates in Flow Cells by the Limiting Current Technique*", *AIChE Symposium Series* 204, Vol. 77, pp. 75-87, 1981
13. Rohan Akolkar and Uziel Landau, "A Time-Dependent Transport-Kinetics Model for Additives Interactions in Copper Interconnect Metallization", Accepted for publication, *J. Electrochem. Soc*. 2004.
14. Rohan Akolkar and Uziel Landau, "Additives Interactions During Copper Interconnect Metallization" Paper # 189 C, Topical TK; *Proceedings of the AIChE Annual Meeting*, San-Francisco, CA, Nov 16-21 (2003).
15. David Roha and Uziel Landau, *"Transport Controlled Leveling Plating Additives: Steady-State Model for Blocking Additives," J. Electrochem. Soc.,* 137 (3) 824-834, 1990.
16. Oscar Lanzi, III, Uziel Landau, Jonathan D. Reid and Raymond T. Galasco, *"Effect of Local Kinetic Variations on Through-Hole Plating," J. Electrochem. Soc.,* 136 368-374, 1989.

17. Uziel Landau, Eugene Malyshev, Rohan Akolkar, and Sergey Chivilikhin, “Simulations of ‘Bottom-Up’ Fill In Via Plating Of Semiconductor Interconnects”, Paper 189 d, session TK; *Proceedings of the AIChE Annual Meeting,* San-Francisco, CA, Nov 16-21 (2003).

18. Eugene Malyshev, Uziel Landau, and Sergey Chivilikhin, “Modeling The Deposit Thickness Distribution In Copper Electroplating Of Semiconductor Wafer Interconnects”, Paper 190 c, session TK; *Proceedings of the AIChE Annual Meeting*, San-Francisco, CA, Nov 16-21 (2003).

19. R. Caban and T. W. Chapman, *J. Electrochem. Soc.,* **124** (9), 1371-1379 (1977).